Molecular Cell
Article

Alternative Splicing Regulates Biogenesis of miRNAs Located across Exon-Intron Junctions

Ze'ev Melamed,[1] Asaf Levy,[1,3,5] Reut Ashwal-Fluss,[4] Galit Lev-Maor,[1] Keren Mekahel,[1] Nir Atias,[2] Shlomit Gilad,[3] Roded Sharan,[2] Carmit Levy,[1] Sebastian Kadener,[4,*] and Gil Ast[1,*]
[1]Department of Human Molecular Genetics and Biochemistry, Sackler Faculty of Medicine
[2]Blavatnik School of Computer Science
Tel Aviv University, Tel Aviv 69978, Israel
[3]Rosetta Genomics Ltd., 10 Plaut Street, Rehovot 76706, Israel
[4]Department of Biological Chemistry, The Alexander Silberman Institute of Life Sciences, The Hebrew University of Jerusalem, Edmond J. Safra Campus, Givat-Ram, Jerusalem 91904, Israel
[5]Present address: Department of Molecular Genetics, Weizmann Institute of Science, Rehovot 76100, Israel
*Correspondence: skadener@gmail.com (S.K.), gilast@post.tau.ac.il (G.A.)
http://dx.doi.org/10.1016/j.molcel.2013.05.007

SUMMARY

The initial step in microRNA (miRNA) biogenesis requires processing of the precursor miRNA (pre-miRNA) from a longer primary transcript. Many pre-miRNAs originate from introns, and both a mature miRNA and a spliced RNA can be generated from the same transcription unit. We have identified a mechanism in which RNA splicing negatively regulates the processing of pre-miRNAs that overlap exon-intron junctions. Computational analysis identified dozens of such pre-miRNAs, and experimental validation demonstrated competitive interaction between the Microprocessor complex and the splicing machinery. Tissue-specific alternative splicing regulates maturation of one such miRNA, miR-412, resulting in effects on its targets that code a protein network involved in neuronal cell death processes. This mode of regulation specifically controls maturation of splice-site-overlapping pre-miRNAs but not pre-miRNAs located completely within introns or exons of the same transcript. Our data present a biological role of alternative splicing in regulation of miRNA biogenesis.

INTRODUCTION

MicroRNAs (miRNAs) are small RNAs of approximately 22 nucleotides (nt) that play important roles in posttranscriptional regulation of gene expression. miRNAs recognize complementary sequences in the 3′ untranslated region (UTR) of their target messenger RNAs (mRNAs) (Kim, 2005) and repress translation or diminish their half-lives (Bartel, 2009; Filipowicz et al., 2008). Most miRNAs are produced from either intergenic or intronic regions of coding or noncoding genes (Rodriguez et al., 2004; Saini et al., 2007) and are transcribed primarily by RNA polymerase II (pol II) as part of longer primary miRNA (pri-miRNA) transcripts that are capped, spliced, and polyadenylated (Cai et al., 2004; Lee et al., 2004). The first step in pri-miRNA maturation is carried out in the nucleus by the Microprocessor complex, containing the RNase III enzyme Drosha and its cofactor DGCR8. This step produces the precursor miRNA hairpin (pre-miRNA) (Denli et al., 2004; Han et al., 2004). The pre-miRNA is exported to the cytoplasm by the Exportin-5/RanGTP complex where it is cleaved by Dicer to generate the miRNA:miRNA* duplex (Lund et al., 2004; Yi et al., 2003). The mature miRNA strand is then preferentially incorporated together with the Argonaute proteins (AGO2) into the RNA-induced silencing complex, or RISC (Winter et al., 2009).

miRNA maturation is regulated at multiple levels, both in the nucleus and in the cytoplasm (Krol et al., 2010). Cleavage of pri-miRNAs by Drosha occurs cotranscriptionally (Morlando et al., 2008; Pawlicki and Steitz, 2008); however, discrepancies between the levels of the pri-miRNA transcript and pre-miRNAs have been documented, suggesting that production of pre-miRNAs is regulated (Siomi and Siomi, 2010). Differential processing of pre-miRNAs into mature miRNAs also leads to tissue-specific and developmental-specific miRNA expression in mammals (Heo et al., 2009; Levy et al., 2010).

Like the initial step of miRNA processing, RNA splicing occurs cotranscriptionally in the nucleus (Kornblihtt, 2007; Luco et al., 2011). The spliceosome cleaves the precursor mRNA (pre-mRNA) molecule, excises introns, and ligates exons to generate a mature mRNA. Alternative splicing (AS) enables the generation of various mRNA molecules from a single gene unit, thereby increasing transcriptomic diversity. Alternatively spliced isoforms are often associated with specific tissues or developmental stages (Braunschweig et al., 2013).

The majority of mammalian miRNAs are located within introns (Golan et al., 2010; Kim and Kim, 2007), and their expression is correlated with the expression of the spliced RNA derived from the host transcript (Baskerville and Bartel, 2005; Wang et al., 2009). It has been demonstrated that splicing is not a prerequisite for processing of intronic miRNAs (Kim and Kim, 2007). Cleavage of intronic miRNAs is thought to occur more rapidly than splicing. However, the Microprocessor complex is associated with spliceosome components on RNA transcripts that

are both spliced and processed into miRNAs (Kataoka et al., 2009). In addition, there is evidence that splicing and processing of intronic miRNAs may affect each other (Janas et al., 2011; Yan et al., 2012).

Here, we identified a class of miRNAs with precursors that are located across active splice sites. Bioinformatics analyses revealed dozens of miRNAs from vertebrates and invertebrates, including human, that share this intriguing genomic location. We demonstrated that the position of pre-miRNAs across splice-site regions results in a competitive interaction between the splicing machinery and the Microprocessor complex. We present evidence that the biogenesis of pre-miRNAs located across splice sites is regulated by AS. Exon inclusion negatively regulated maturation of the splice site overlapping miR-412, whereas cotranscribed miRNAs located within intronic or exonic regions were not affected by this splicing event, providing additional insight into the regulation of expression of miRNAs in polycistronic clusters. Manipulation of the levels of the Microprocessor components, Drosha and DGCR8, showed that miRNA processing modulates AS of exons that overlap pre-miRNAs. Finally, high-throughput analysis of mRNA bound to the AGO2 complex (RIP-Chip) identified a set of miR-412 target genes that are involved in neuronal cell death processes. Levels of these mRNA targets were positively correlated with inclusion of the miR-412 overlapping exon in vivo, indicating that regulation of miRNA biogenesis by AS has a bona fide biological role.

RESULTS

Computational Identification and Characterization of Pre-miRNAs Located across Exon-Intron Junctions

We conducted a large-scale bioinformatic analysis of the genomic locations of miRNA precursors within hosting genes of four invertebrate and 14 vertebrate species. We identified 52 pre-miRNAs located across exon-intron junctions of aligned spliced expressed sequence tags (ESTs) or mRNAs. Splice-site-overlapping miRNAs were more often found in mammalian genomes (n = 45, 87%) than in those of other species, and 46% (n = 24) were in the human genome (Table S1 available online). We assumed that, if the spliceosome and the Microprocessor complex operate on the same region on the RNA transcript, then the maturation of these miRNAs might be inhibited by the splicing process, which should cleave the transcript within the pre-miRNA sequence.

We characterized the conservation, coding potential, and splicing patterns of the splice junction miRNA hosting genes (Table S1). For 20 miRNAs, there is evidence of orthologous transcripts (Table S1). In most cases (17/20), the location of the pre-miRNA sequences across a splice junction was not conserved, although the miRNAs identified are conserved in mammals (see Supplemental Results and Discussion; Figure S1A). For example, the pre-miR-202 in mouse is located fully within an exon (Figure S1B), whereas in human it lies across a splice junction (Figure S1C). This implies that human miR-202 is exposed to a negative regulation by splicing, whereas murine miR-202 is not.

We analyzed expression patterns of splice-site-overlapping miRNAs (Table S1) and identified several intriguing genes in which a splice-site-overlapping miRNA is cotranscribed with other exonic/intronic miRNAs. Of note, miRNA expression data based on deep-sequencing studies (Griffiths-Jones et al., 2008) clearly demonstrate that the numbers of reads that mapped to the splice-site-overlapping miRNAs are exceptionally low relative to numbers of reads representing cotranscribed intronic or exonic miRNAs (see Supplemental Results and Discussion; Figure S1D). For example, the splice-site-overlapping mmu-miR-412 is transcribed as a part of a long noncoding RNA gene (Mercer et al., 2008), *Mirg*, which contains nine additional miRNA precursors. We observed 2,198 reads corresponding to miR-412 and 172,109 reads and 46,771 reads from intronic miR-541 and exonic miR-410, respectively (Griffiths-Jones et al., 2008). These observations imply that, when a pre-miRNA is positioned as part of a splice site, less of the mature miRNA is produced than when the pre-miRNA is located within an intron or exon.

AS Is Inversely Correlated with Levels of miR-412 In Vivo

To confirm that splicing and processing of pre-miRNAs located across exon-intron junctions are mutually exclusive, we selected the *Mirg* cluster for further analysis. miR-412 overlaps the 3′ splice site (3′ss) of an exon that is predicted to be alternatively spliced (Figure 1A); cotranscribed miRNA precursors are either intronic or exonic. Therefore, we used this unique miRNA cluster combining several types of miRNAs as a platform to study the interaction between miRNA processing and RNA splicing. Figure 1B illustrates the genomic region of miR-412 and selected miRNAs that also reside in the cluster. We first sought to validate that the predicted alternatively spliced exon was incorporated into mature RNA. We found that the inclusion level of the alternative exon varied across adult and embryonic mouse tissues (Figure 1C). Since the hosting gene, *Mirg*, is a noncoding gene, we hypothesized that tissue-specific regulation of the alternative exon has an atypical biological function in these tissues. Sequencing of the exon-inclusion isoform demonstrated that the alternative exon contains the 3′ end of the pre-miR-412 hairpin, confirming that exon inclusion eliminates production of the miR-412 precursor. In other mouse tissues examined (heart, kidney, and pancreas), *Mirg* transcripts were not detected or were detected at very low levels, suggesting that transcriptional regulation impacts the biogenesis of miRNAs from the *Mirg* cluster.

Previous reports demonstrated that the noncoding *Mirg* gene is mainly expressed in the murine brain (Han et al., 2012; Mercer et al., 2008), and our computational analysis supported this (Table S1). To determine whether inclusion of the alternative exon negatively affected the biogenesis of miR-412, we focused on adult brain and embryonic brain tissues, which had clear differences in the splicing patterns of *Mirg* transcripts. We examined the expression levels of intronic miR-541, miR-412 located across the exon-intron junction, and exonic miR-410 using a quantitative real-time PCR assay (qPCR). The levels of intronic miR-541 were essentially the same in embryonic and adult brain tissues (Figure 1D). In contrast, the level of miR-412 was more than 2-fold higher in embryonic brain tissue than in adult brain tissue ($p < 0.05$), indicating that exon inclusion is inversely correlated with expression level of the overlapping miR-412. Levels of exonic miR-410 in embryonic brain tissue were lower than in

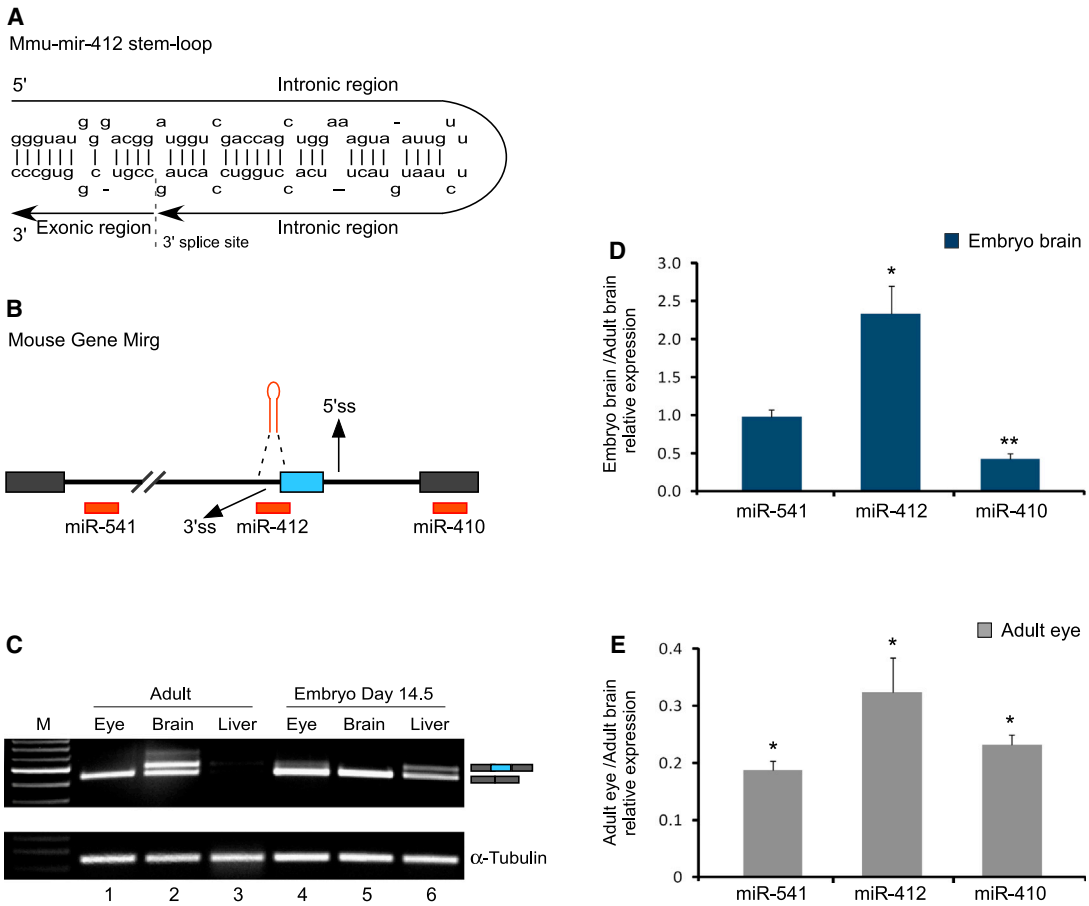

Figure 1. Negative Correlation between Exon Inclusion and miR-412 Expression In Vivo

(A) Predicted secondary structure of the precursor miR-412. Arrows indicate 5′ to 3′ direction.

(B) Diagram of the miR-412 genomic region. The black boxes represent exons; the blue box represents the middle alternatively spliced exon. The genomic locations of pre-miR-412 and two selected miRNAs from the cluster are marked with red lines.

(C) Endogenous expression of the *Mirg* gene (upper panel). Exon inclusion and skipped isoforms are shown to the right of the gel; α-tubulin was used as an internal control (lower panel).

(D and E) Endogenous expression of selected miRNAs from the cluster in the indicated tissues relative to the adult brain tissue; (D) shows embryo brain, and (E) shows adult eye. *$p < 0.05$. **$p < 0.1$ (t test, n = 3). Error bars represent SEM. See also Figures S1 and S2.

adult brain tissue ($p < 0.1$). Using primers that flank miR-410 hosting exon, we found that this exon was constitutively spliced, suggesting that changes in levels of miR-410 are not due to splicing of its hosting exon (data not shown). It is interesting that the expression level of *Mirg* in the adult brain tissue was significantly higher than in the embryonic brain (Figures S2D–S2E). These results imply that, although the *Mirg* gene is transcribed at higher levels in adult brain tissue, inclusion of the alternative exon interferes with the biogenesis of miR-412, whereas exon skipping in the embryonic brain tissue allows efficient cleavage of pre-miR-412.

We then compared the levels of these miRNAs in adult eye tissue, in which the exon was skipped, and adult brain tissue, in which the exon was alternatively spliced. All three miRNAs were significantly downregulated in the eye tissue relative to the brain tissue ($p < 0.05$; Figure 1E). Levels of the three miRNAs were not decreased by the same amounts: miR-412 was downregulated by about 3-fold in eye tissue, whereas miR-541 and miR-410 levels were decreased at least 5- and 4-fold, respectively. This suggests that a posttranscriptional mechanism differentially affects the expression of miRNAs within this cluster. A computational analysis comparing miR-412 expression and alternative exon inclusion levels in 11 mouse tissues indicated that there is a competition between miRNA biogenesis and alternative exon selection (see Supplemental Results and Discussion; Figure S2).

Exon Inclusion Specifically Impacts Levels of miR-412

To further validate that splicing is directly involved in the regulation of miR-412 biogenesis, we generated a plasmid carrying the genomic region of the murine miR-412, composed of three exons and two introns (Figure 1B). The plasmid was transfected into human 293T cells that lack corresponding endogenous miRNAs, and the splicing pattern of the transcripts generated

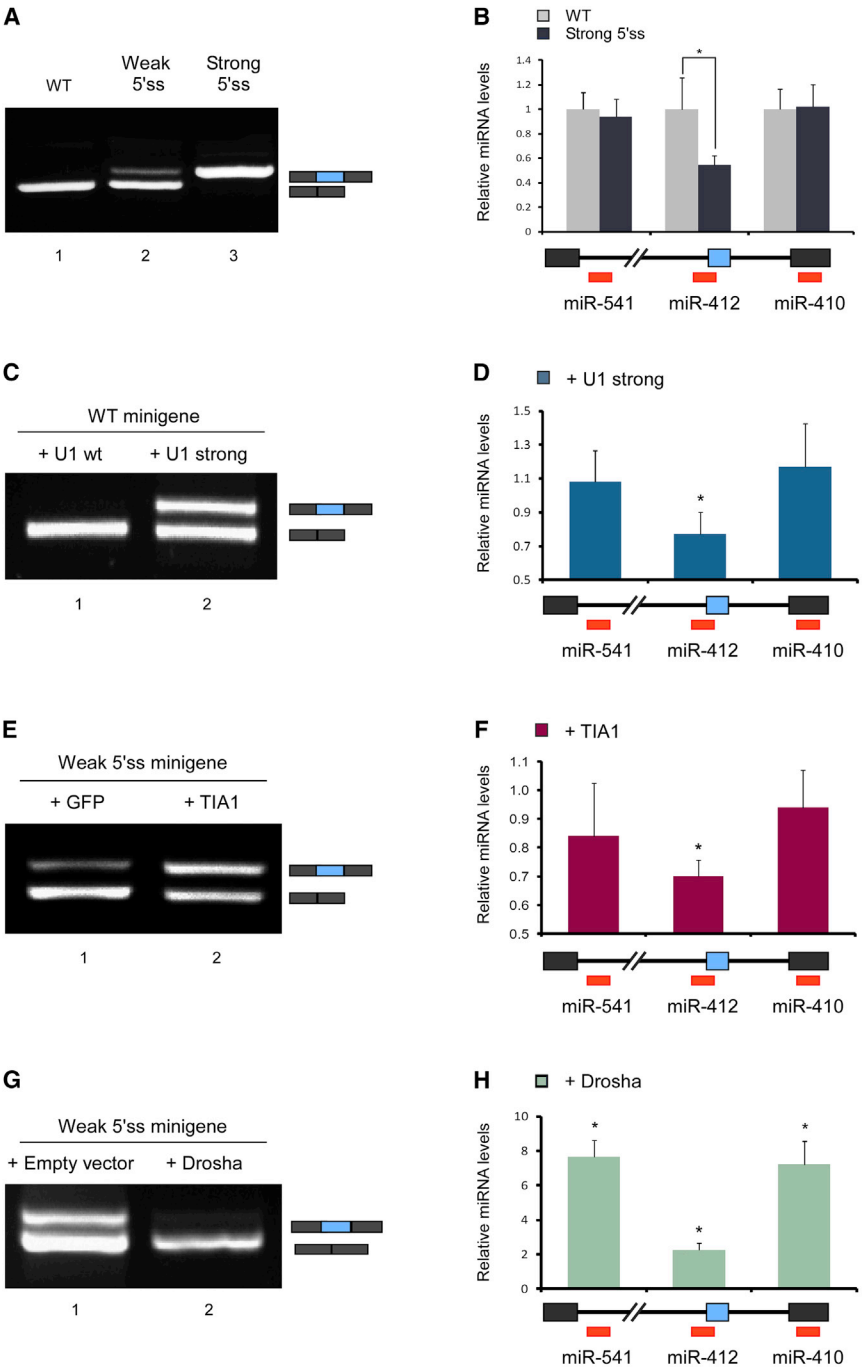

Figure 2. Splicing and Drosha Levels Affect miRNA Maturation

(A) Splicing pattern of the WT *Mirg* minigene (lane 1) and plasmids containing weak and strong mutations in the 5′ss (lanes 2 and 3, respectively).

(B) qPCR of mature miRNAs from WT (light gray) and strong 5′ss (dark blue) constructs was calculated using qPCR analysis.

(C) Splicing pattern of the WT *Mirg* minigene following cotransfection with U1 WT (lane 1) or a U1 mutant that enhances base paring to the 5′ss (U1 strong; lane 2).

(D) qPCR of mature miRNAs from the *Mirg* constructs following cotransfection with U1 strong relative to cotransfection with WT U1.

(E) Splicing pattern of the "weak 5′ss" *Mirg* minigene following cotransfection with GFP (lane 1) or vector encoding TIA1 (lane 2).

(F) qPCR of mature miRNAs following cotransfection with TIA1 vector.

(G) Splicing pattern of the "weak 5′ss" *Mirg* minigene following cotransfection with an empty plasmid (lane 1) or a plasmid encoding Drosha (lane 2).

(H) qPCR of mature miRNAs from the *Mirg* constructs following cotransfection with plasmid encoding Drosha relative to cotransfection with Drosha mutant.

For (B), (D), (F), and (H), expression of each miRNA was normalized to U6B snRNA (t test, $p < 0.05$; $n = 3$). Error bars represent SEM. See also Figure S3.

from the minigene were examined. In the wild-type (WT) minigene, the middle exon was skipped, as confirmed by sequencing (Figure 2A, lane 1). In order to enhance inclusion of the alternative exon without changing the pre-miRNA sequence, we designed mutations in the 5′ splice site (5′ss) that enhance U1 small nuclear RNA (snRNA) base pairing; this pre-miRNA overlaps the 3′ss. Mutation of the splice site from gtactt to gtgggt, a "weak" mutation, elevated levels of inclusion slightly, whereas the "strong" mutation, gtactt to gtaagt, resulted in constitutive splicing (Figure 2A, lanes 2 and 3, respectively). Levels of miRNAs obtained from the "weak" minigene were not significantly different from those obtained from the WT minigene (data not shown). In contrast, the level of miR-412 from the "strong" minigene was significantly reduced ($p < 0.05$), although levels of intronic miR-541 and the exonic miR-410 were unchanged (Figure 2B). These results suggest that the splicing machinery directly regulates the biogenesis of miR-412 through regulation of the inclusion level of the alternative exon, while other miRNAs within the same cluster are not affected. Additional experiments (Figures S3A–S3E) demonstrate that this effect is indeed caused by the shift in splicing and not due to unrelated inhibition of miRNA biogenesis.

The involvement of U1 snRNA in AS regulation has been documented (Buratti and Baralle, 2010; Keren-Shaul et al., 2013; Roca et al., 2013), and our results (Figures 2A and 2B) led us to suspect that regulation of U1 binding to the 5′ss region modulates exon selection and affects miR-412 levels. To test this hypothesis using a different strategy, we cotransfected the *Mirg*-derived WT minigene and a plasmid expressing U1 snRNA

into cells. This U1 snRNA contains compensatory mutations that strengthen U1 snRNA base pairing with the 5′ss of the internal exon (Figure S3F). Improving binding of U1 snRNA to the 5′ss raised the inclusion levels of the internal exon from skipping to alternative selection (Figure 2C) and, consequently, decreased the production of miR-412 by the Microprocessor complex ($p < 0.05$; Figure 2D). Thus, binding of a splicing factor on the transcript far from pre-miR-412 affected its processing.

Noncanonical base pairing of U1 snRNA to 5′ss region can be mediated by splicing regulatory proteins that facilitate spliceosome assembly (Long and Caceres, 2009). To explore how splicing of miR-412 overlapping exon is regulated, we utilized the WASP tool (Barash et al., 2010) to identify potential *cis*-acting regulatory elements in proximity to the alternative exon region. We found putative binding sites for the TIA proteins, a previously described family of splicing factors that promote recognition of weak 5′ss (Gal-Mark et al., 2009; Le Guiner et al., 2001; Wang et al., 2010). To explore the potential association between TIA and the miR-412 genomic region, we cotransfected the minigene in which the exon is alternatively spliced with a plasmid that contains the cDNA encoding TIA1 (Del Gatto-Konczak et al., 2000). We observed a significant increase in the inclusion level of the internal exon (Figure 2E), suggesting that functional U1 snRNA base pairing with the 5′ss is mediated by the activity of TIA1. The increase in exon selection was validated by qPCR analysis (Figure S3G). In addition, we found that the levels of miR-412 were significantly decreased ($p < 0.05$), whereas intronic miR-541 and exonic miR-410 exhibited no significant changes in their expression levels (Figure 2F). Together, these results provide compelling evidence that regulation of 5′ss recognition by the splicing machinery affects the biogenesis of the 3′ss-overlapping miR-412.

Overexpression of Drosha Differentially Affects Maturation of miRNAs in the *Mirg* Cluster

The reduction in miR-412 levels upon exon inclusion implies that Drosha competes with the splicing machinery for processing of a common RNA transcript. In order to better understand this competition, we sought to examine the role of Drosha in the expression of different miRNAs in the *Mirg* cluster. For this analysis, we used the minigene in which the exon is alternatively spliced (Figure 2A, lane 2), since it represents an intermediate level of competition between the two machineries. We cotransfected this minigene with plasmids that contained cDNA for Drosha or a mutated Drosha (Han et al., 2009). Quantification of mature miRNAs showed that overexpression of Drosha increased levels of the intronic and the exonic miRNAs (miR-541 and miR-410, respectively) by more than 7-fold but had a much more modest effect (2- to 3-fold) on the expression of miR-412 (Figure 2H). The effect of Drosha on the levels of miRNAs in the cluster was higher than expected but may be explained by the use of a dominant negative mutant Drosha as a control. These results demonstrate that the genomic location of miRNAs is an important factor in the regulation of their biogenesis. Furthermore, overexpression of Drosha significantly reduced the levels of spliced *Mirg* transcripts (Figure 2G), whereas introduction of a Drosha mutant caused the opposite effect (Figure S3H). We hypothesize that enhanced cleavage of miRNAs from the *Mirg* cluster, and particularly of the exonic miR-410, led to degradation of the hosting transcripts and reduced levels of the spliced RNA isoforms.

Pre-miRNA Secondary Structure Interferes with Splice Site Recognition

To obtain further evidence for the competition between the splicing machinery and Microprocessor complex, we experimentally examined the regulation of human miR-202. The precursor for miR-202 overlaps the 5′ss of an alternatively spliced exon (Figure 3A). We generated a plasmid carrying the hosting gene of human miR-202, including three exons separated by two introns (Figure 3B), and transfected it into 293T cells that do not express mature miR-202 (data not shown). Upon expression of the miR-202 minigene in 293T cells, the central exon was invariably skipped (Figure 3C, lane 1) as confirmed by sequencing. Since pre-miR-202 is located across the 5′ss, we strengthened the polypyrimidine tract (PPT) region of the alternative exon by mutagenesis from gtg to ttt. Strengthening of the PPT led to incorporation of the exon that overlaps pre-miR-202 (Figure 3C, compare lane 1 and lane 2). Concomitantly, the level of the skipped isoform was significantly reduced, demonstrating a shift in splicing toward exon inclusion ($p < 0.05$; Figure 3D). Sequencing of the splice variants in which the alternative exon was included confirmed that exon inclusion destroys the miR-202 hairpin, as 67 nt of the pre-miR-202 (61% of its length) is incorporated into the spliced transcript. As expected, the levels of miR-202 were significantly reduced in samples in which the exon was included compared to those in which the exon was skipped ($p < 0.05$; Figure 3E). We then generated an additional minigene containing mutations at the PPT site that did not alter exon selection. These mutations did not affect expression level of miR-202 (Figures S4A–S4C). Our results indicate that the splicing machinery is able to modulate the levels of miRNAs that overlap with both the 3′ss (mmu-miR-412) and the 5′ss (hsa-miR-202).

In the miR-202 minigene, mutations that strengthened the 5′ss slightly (gtatag to gtatgg) or strongly (gtatag to gtatgt) did not improve exon inclusion (Figure S4D, lanes 1 and 2, respectively). We hypothesized that exon selection was not improved due to 5′ss mutations because the stem structure of pre-miR-202 sequesters the 5′ss and blocks binding of U1 snRNA to that region. To test this hypothesis, we generated mutations designed to destabilize the pre-miRNA stem structure without altering the strength of the 5′ss signal (see Supplemental Information). This destabilization of the pre-mRNA structure led to exon recognition and AS of the central exon of the minigene transcript (Figure 3F, compare lanes 1 and 2) and reduced levels of miR-202 (data not shown). We also coupled the hairpin disrupting mutations with a mutation that strengthened the 5′ss (the same mutation as in Figure S4D, lane 2). Notably, this combination led to constitutive selection of the internal exon (Figure 3F, lane 3). An intermediate splicing isoform that contains the alternative exon together with the upstream intron (intron retention) was also detected. These results indicate that the stem-loop structure of miR-202 sequesters the 5′ss and inhibits processing by the splicing machinery. Destabilization of the stem structure gave the advantage to the splicing machinery and may have

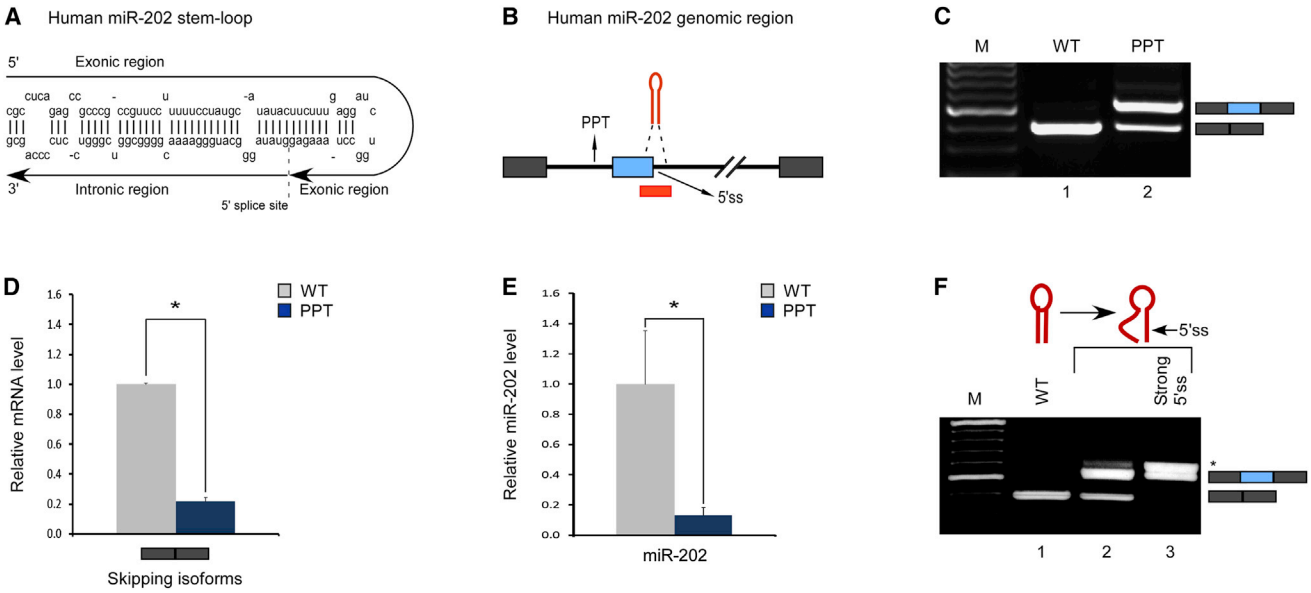

Figure 3. Expression of Human miR-202 Is Subject to Competition between RNA Splicing and miRNA Processing

(A) Predicted secondary structure of the pre-miR-202 stem-loop. Arrows indicate 5′ to 3′ direction of the pre-miRNA.

(B) Diagram of the miR-202 minigene.

(C) Splicing pattern of the WT miR-202 minigene (lane 1) and miR-202 minigene with mutation in PPT (lane 2).

(D) qPCR of the skipping isoforms produced from miR-202 minigenes following the transition from exon skipping (WT, light gray) to alternative selection (mutant, dark blue) (t test, $p < 0.05$; $n = 3$). Error bars represent SEM.

(E) qPCR of mature miR-202 following the transition from exon skipping (WT, light gray) to alternative selection (mutant, dark blue) (t test, $p < 0.05$; $n = 3$). Error bars represent SEM.

(F) Splicing pattern of miR-202 minigene following disruption of miR-202 hairpin structure. Lane 1, splicing products of WT minigene. Lane 2, splicing products following mutations to destabilize the pre-miR-202 hairpin structure. Lane 3, splicing products following destabilization of the hairpin and strengthening of the 5′ss (as in Figure 4F, lane 2). An asterisk indicates that the uppermost band retains a short upstream intron as confirmed by sequencing. See also Figure S4.

altered the ability of the Microprocessor complex to bind to the miRNA stem-loop structure. Therefore, we assume that the balance between affinity of the spliceosome components and the Microprocessor complex for a transcript might determine the execution of each process.

Expression Levels of Drosha and DGCR8 Modulate Inclusion of Exon that Overlaps the miRNA Precursor Region

The interaction between the Microprocessor complex and the pri-miRNA molecule is mediated mainly by the RNA binding protein DGCR8, which recognizes the stem-loop structure of the pre-miRNA and recruits Drosha to its cleavage site (Han et al., 2006). To test whether DGCR8 levels impact the competition between the spliceosome and the Microprocessor complex, we cotransfected the miR-202 minigene in which the exon is alternatively spliced and a plasmid for expression of DGCR8 into 293T cells. Overexpression of DGCR8 significantly reduced inclusion of miR-202 overlapping exon and caused a shift in the splicing pattern toward exon skipping (Figure 4A). This was validated by qPCR analysis (Figure 4B). Levels of mature miR-202 were significantly elevated, indicating enhanced Microprocessor activity (Figure 4C). These results demonstrate that higher levels of DGCR8 tilt the balance in favor of miR-202 processing over splicing of the alternative exon. We also examined the impact of Drosha under these conditions; as expected, overexpression of Drosha significantly reduced the inclusion of the alternatively spliced exon (Figure S5, compare lanes 2 and 3). Together, these results support the hypothesis that the Microprocessor complex and the spliceosome compete for binding to the same RNA region in the pri-miR-202 hairpin structure.

We next evaluated splicing of the miR-202 minigene after RNA interference-mediated knockdown of Drosha. Small interfering RNA (siRNA) targeted against *drosha* mRNA caused a marked change in the splicing pattern of miR-202 overlapping exon (Figure 4D). Levels of skipping variants were significantly decreased, whereas inclusion of the alternative exon was induced (Figure 4E). mRNA and protein levels of Drosha were significantly reduced under these conditions (Figures 4F and 4G, respectively). These results indicate that the reduction in Drosha levels allowed more efficient recognition by the spliceosome of the splice site overlapped by miR-202. These results also confirmed that each RNA molecule can undergo either miRNA processing or AS; therefore, selection of this exon decreases miR-202 levels.

Location across a 3′ss Impairs miRNA Biogenesis

To examine the effect of splice site environment upon biogenesis of adjacent miRNA, we generated a construct containing the genomic region of the hsa-miR-365-2, including two exons separated by one intron (Figure 5A). There are two genomic copies of the human miR-365 precursor that yield identical

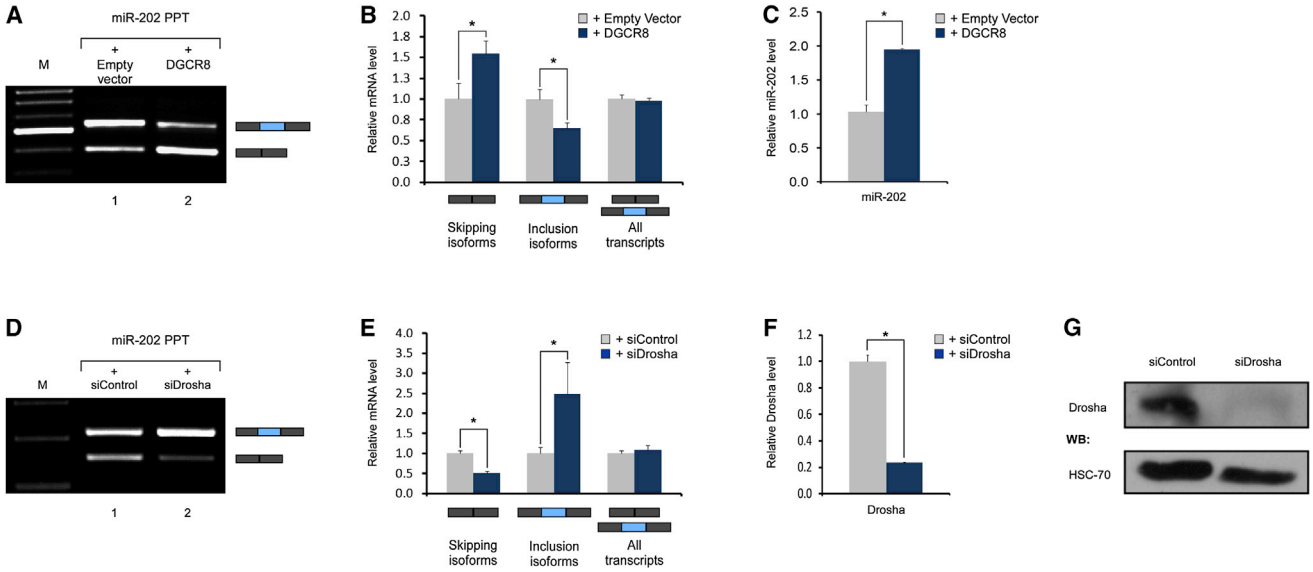

Figure 4. Levels of Microprocessor Components Modulate Alternative Splicing

(A) Splicing pattern of the mir-202 minigene following cotransfection with an empty plasmid (lane 1) or plasmid containing cDNA encoding DGCR8 (lane 2).

(B) qPCR of spliced isoforms expressed from miR-202 minigenes following cotransfection with a plasmid encoding DGCR8 (blue) or an empty plasmid (light gray) (as in Figure 4A). Error bars represent SEM (t test, $p < 0.05$, $n = 3$).

(C) qPCR of mature miR-202 level following overexpression of DGCR8 (as in Figure 4A). Error bars represent SEM (t test, $p < 0.05$; $n = 3$).

(D) Splicing pattern of the mir-202 minigene following Drosha knockdown (siDrosha, Ambion) in 293T cells. Scrambled siRNA was used as a positive control (siControl, lane 1).

(E) qPCR of spliced isoforms produced from miR-202 minigenes following treatment of cells with siControl (light gray) or siDrosha (blue).

(F) qPCR analysis of *drosha* mRNA levels following treatment with siControl (light gray) or siDrosha (blue). For (E) and (F), error bars represent SEM (t test, $p < 0.05$; $n = 3$).

(G) Western blot analysis following Drosha knockdown was performed using antibodies directed against Drosha (Upstate; #07-717) or HSP70 as a loading control. See also Figure S5.

mature miRNAs. Hsa-miR-365-1 is located in the intron of its hosting gene, and its expression should not be impacted by splicing, whereas hsa-miR-365-2 is located across an exon-intron boundary. We transfected the miR-365-2 vector into 293T cells, extracted RNA, and demonstrated by RT-PCR and sequencing of the product that the putative splice site was recognized (Figure 5B, lane 1). We then activated a downstream cryptic 3′ss by mutagenesis so that miR-365-2 was no longer located across the preferred 3′ss. RT-PCR analysis indicated that the cryptic 3′ss was used in more than 90% of processed transcripts (Figure 5B, lane 2). Using qPCR analysis, we examined the expression of miR-365-2 from the mutant and the WT minigenes. Levels of miR-365-2 were significantly higher in the mutant containing the activated cryptic 3′ss ($p < 0.05$; Figure 5C), suggesting that the stem-loop structure is more efficiently cleaved by the Microprocessor complex in the intronic environment in which the competition with the splicing machinery is diminished. These results also suggest that appearance of an active splice site within a pri-miRNA during evolution can serve as a means for decreasing the levels of miRNA expression.

miR-412 Is a Functional miRNA Targeting mRNAs via RISC

To determine whether the regulation of splice-site-overlapping miRNA via AS has a biologically meaningful role, we concentrated on miR-412 whose expression in brain tissues was confirmed here and in previous reports (Chiang et al., 2010). Since no mRNA targets of miR-412 have been identified, we first evaluated the association of miR-412 with mRNA in RISC (Figure S6A). We cotransfected a plasmid driving the expression of a Flag-tagged AGO2 protein and either pri-miR-412 or green fluorescent protein (GFP)-expressing plasmids into neuronal N2A cells. Immunoprecipitation (IP) of AGO2 protein-RNA complexes (Peritz et al., 2006) was observed (Figure 6A). We then purified RNA bound to the AGO2 protein complex and found that AGO2 was associated with a number of miRNAs, including let-7c (Figure 6B). miR-412 was enriched about 7-fold in the AGO2-IP fraction of the GFP-transfected cells compared with immunoglobulin G (IgG)-IP fraction (Figure 6B). Thus, endogenous miR-412 is loaded into the RISC. Overexpression of pri-miR-412 resulted in a very significant increase (~90-fold) in levels of mature miR-412 associated with AGO2-IP fraction, representing very efficient loading of the exogenous miRNA (Figure 6B). These results clearly demonstrate that miR-412 is properly processed and loaded into AGO2-containing RISC complexes.

In order to evaluate the ability of miR-412 to recruit mRNA into the RISC, we determined the population of mRNAs bound to AGO2 in control and miR-412-overexpressing cells using Affymetrix microarrays. We then compared the list of mRNAs

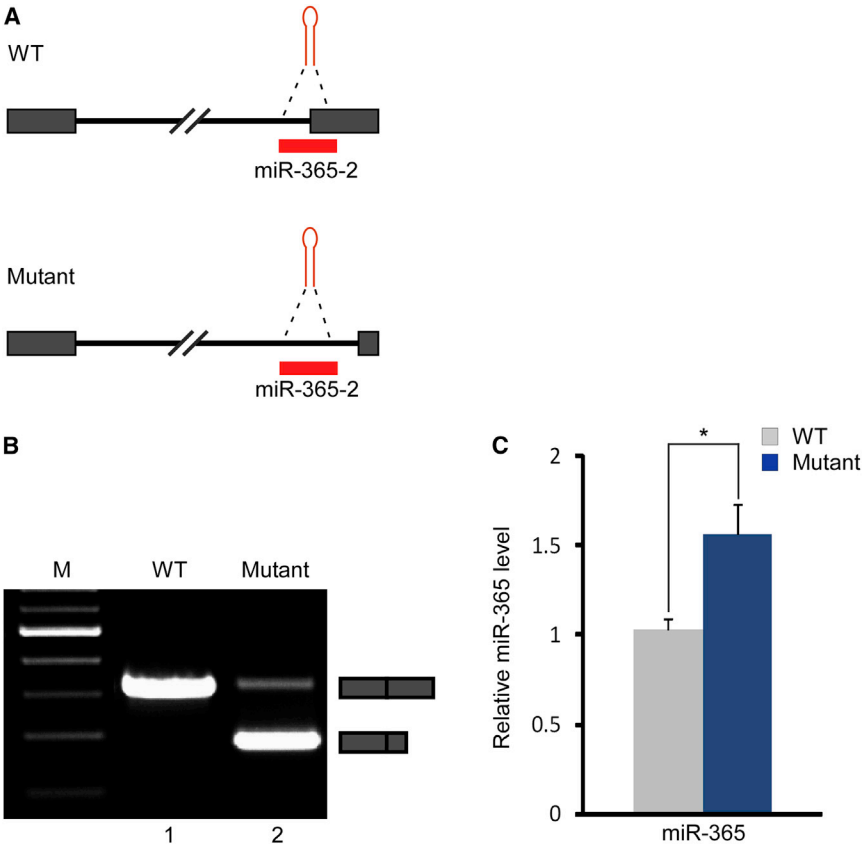

Figure 5. Expression of miR-365-2 Is Enhanced when Located in an Intronic Region Rather Than across a Splice Site

(A) Diagrams of the miR-365 minigenes. The red line and the red hairpin represent the pre-miR-365-2 region.

(B) RT-PCR products of WT minigene (lane 1) or mutated miR-365 minigene (lane 2).

(C) qPCR of miR-365 level in the WT sample (light gray) and in the mutant sample (dark blue) in which the hairpin of miR-365-2 is intronic (t test, $p < 0.05$; $n = 3$). Error bars represent SEM.

enriched in the AGO2 complex with predicted targets of miR-412 retrieved from the miRDB database (http://mirdb.org/miRDB) (Figure 6F, upper scheme). A substantial number of the predicted miR-412 targets (21.1%) were enriched in the AGO2 IP fraction following overexpression of miR-412. To assay the significance of these potential miR-412 targets, we performed a similar calculation for 981 additional murine miRNAs. miR-412 was ranked as 28th of the 981 ($p = 0.028$; Figure 6C), indicating that the identified AGO2-associated mRNAs are likely miR-412 targets. We conclude that strong association of miR-412 with AGO2 complexes significantly influenced the association of the relevant endogenous mRNA targets to the RISC.

Silencing of Genes Involved in Neuronal Cell Death Processes Is Positively Correlated with Inclusion of the miR-412 Overlapping Exon in Vivo

To examine whether miR-412 induces silencing of the identified AGO2-associated mRNAs, we overexpressed miR-412 in N2A cells using a miR-412-GFP construct. Viable GFP-positive cells were isolated by fluorescence activated cell sorting, and levels of ten potential miR-412 targets that demonstrated the highest enrichment score in the AGO2 protein-RNA complexes (Table S2) were examined by qPCR. Levels of eight of ten suspected target genes were significantly downregulated following overexpression of miR-412 (Figures 6D and S6B). To determine whether these AGO2-associated mRNAs are biological targets of miR-412 in vivo, we examined the levels of each of the ten potential targets in embryonic and adult brain tissues, which express different levels of miR-412. In the embryonic brain tissue, the alternative exon is skipped and miR-412 levels are higher than in adult brain tissue in which the exon is included (Figure 1C). It is interesting that the levels of six of ten potential target genes were significantly reduced in the embryonic brain tissue relative to adult tissue (Figures 6E and S6C). Moreover, of those genes displaying inverse correlations with the miRNA, five were directly affected by miR-412 levels in N2A cells (Figure 6D). These results suggest that these genes mediate the biological role of miR-412 in vivo (Figure 6F, lower scheme).

Recent studies suggest that target genes regulated by an individual miRNA generally interact through a network of functionally associated genes (Liang and Li, 2007; Satoh, 2012). We used ANAT (Yosef et al., 2011), a network analysis toolkit, to infer a parsimonious network connecting the most abundant AGO2-mRNA targets for which protein-protein interaction data were available. Of note, six of the ten candidate targets were part of a potential biological network of functionally associated molecules (Figure 6G). Genes that do not appear in the network do not have strong evidence for protein-protein interacting partners. Enrichment analysis of the reconstructed network ($p < 0.001$; false discovery rate corrected) found that both miR-412 potential targets and their associated intermediate node genes were over-represented in programmed cell death processes according to both gene ontology (GO) (see Table S3) and KEGG—Kyoto Encyclopedia of Genes and Genomes—annotations (KEGG apoptosis pathway ID hsa:4210; $p < 1.9 \times 10^{-5}$) (Kanehisa and Goto, 2000). In contrast, the list of all ten candidate target genes was not significantly enriched in any GO category. Notably, among the five miR-412 targets that we experimentally validated in the neuronal cell line (Figure 6D) and in brain tissues (Figure 6E), involvement of the products of four genes—*MAPK9*, *IFT57*, *PPT1*, and *HIPK3*—in neuronal cell death processes is well established (Curtin and Cotter, 2004; Gdynia et al., 2008; Ries et al., 2008; Tardy et al., 2009). Together, these results

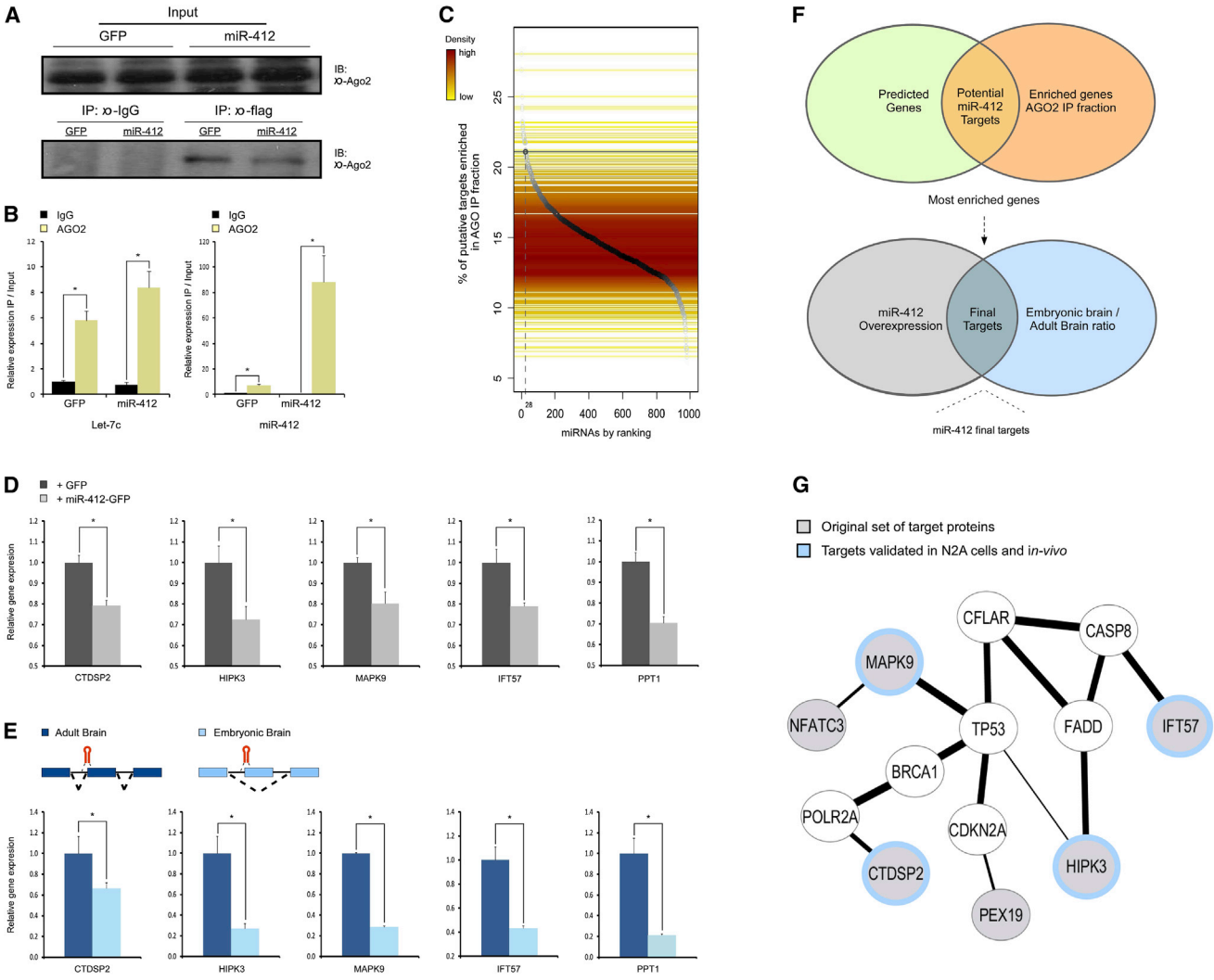

Figure 6. miR-412 Is a Functional miRNA Targeting mRNA via RISC

(A) IP of AGO2-containing complexes was validated by western blot analysis using anti-AGO2 (upper panel; results from duplicate plates). Specific precipitation of AGO2 was confirmed (lower panel).

(B) qPCR of let-7c (left panel) or mir-412 (right panel) in the AGO2 IP fraction relative to the IgG IP fraction. Error bars represent SEM.

(C) Enrichment of AGO2-associated mRNAs. The y axis represents percentage of putative targets enriched in the AGO2-associated mRNAs. The x axis lists miRNAs by enrichment ranking. Dashed line indicates miR-412 score relative to 981 murine miRNAs analyzed (top 3%). Each horizontal line represents the enrichment value of a single miRNA. Lines are darkened according to miRNA densities around enrichment score. Each circle on the graph represents a single miRNA. Bold circle and line indicates miR-412 position.

(D) Direct effect of miR-412 levels on predicted targets. qPCR of five selected genes is plotted (see Figure S6B for extended results). Error bars represent SEM (t test, $p < 0.05$; $n = 3$).

(E) Examination of predicted miR-412 targets in adult and embryonic brain tissues. qPCR of five selected genes is plotted (see Figure S6C for extended results). Error bars represent SEM (t test, $p < 0.05$; $n = 3$).

(F) Schematic illustration of the strategy used to identify miR-412 targets.

(G) Network-based analysis of target proteins. Grey nodes represent the original set of target genes; nodes that are encircled with light blue represent genes that were validated in (E) and (F); inferred genes are marked in white. Edge width corresponds to associated confidence. See also Figure S6.

strongly suggest that the regulation of miR-412 biogenesis by AS has a biological function in adult and embryonic brain tissues. The unique regulatory mechanism in which splicing affects the biogenesis of splice-site-overlapping miR-412 results in developmental stage-specific modulation of the levels of its target genes.

DISCUSSION

In this study, we demonstrated that the splicing machinery competes with the miRNA processing machinery when a pre-miRNA sequence overlaps with an active splice site. We identified 52 miRNAs that share this intriguing location in vertebrate and

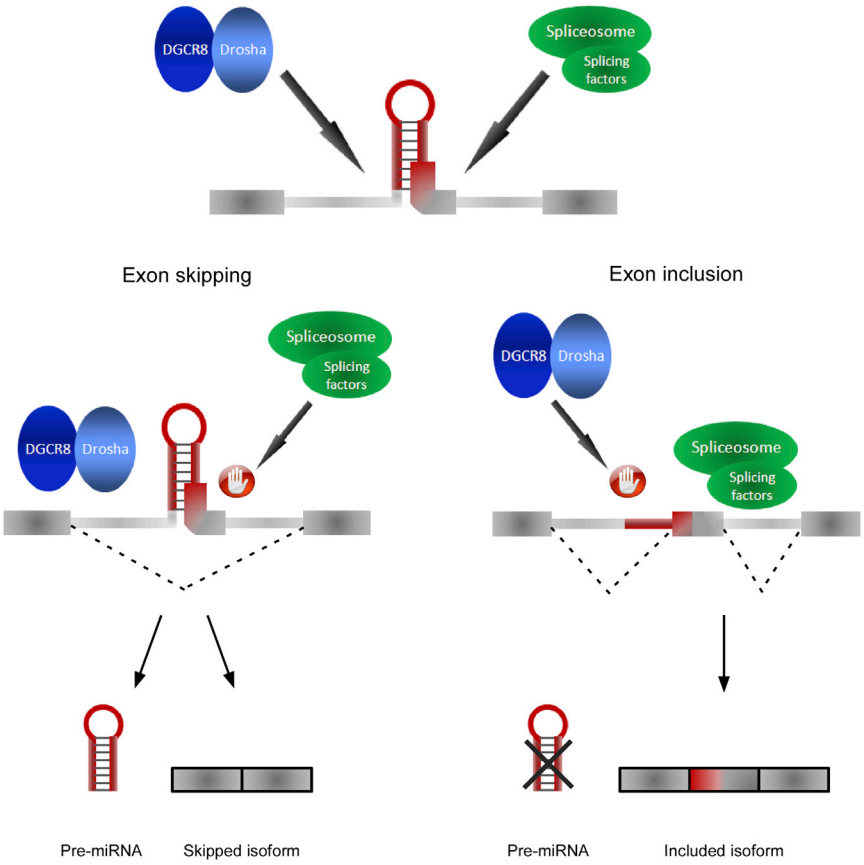

Figure 7. A Regulatory Model of Splice-Site-Overlapping miRNA Biogenesis via AS

The spliceosome and the Microprocessor complex compete for processing of the same RNA region, leading to two possible scenarios. In the left panel, processing of pre-miRNA that overlaps splice junction occurs when the splicing machinery does not recognize the internal exon, and the Microprocessor components—rather than the spliceosome complex—bind to the RNA transcript at the pre-miRNA region. Both skipped isoform and the pre-miRNA can be generated. In the right panel, when the internal exon is recognized through interaction with specific splicing factors, the RNA secondary structure is released and splicing of the internal exon is carried out by the spliceosome before DGCR8 and Drosha bind to the pre-miRNA region. The spliced variant containing the alternative exon is the product and no pre-miRNA is made. See also Figure S7.

nonvertebrate genomes. By manipulating the balance between the splicing machinery and the Microprocessor components, we experimentally validated bidirectional competition in three different cases of splice-site-overlapping miRNAs. We also found evidence that tissue-specific AS of the noncoding gene, *Mirg*, specifically impacts maturation of miR-412. Our data indicate an atypical biological function of AS in regulation of miRNA biogenesis.

In addition to the cases experimentally validated here, other miRNAs were identified at active splice sites of coding genes (Table S1). We suggest that these miRNAs likely serve as negative regulators of their hosting genes as the mRNA transcripts are cleaved by Drosha during miRNA biogenesis rather than through the canonical miRNA gene silencing pathway (Chong et al., 2010; Han et al., 2009; Kadener et al., 2009; Karginov et al., 2010; Macias et al., 2012). In addition, our data suggest that the interplay between splicing and miRNA biogenesis can modulate the expression of paralogous miRNAs that have two distinct genomic copies, one overlapping an active splice site and the other intronic or exonic (see Supplemental Results and Discussion; Figures S7A–S7D).

The first step of processing of certain miRNAs, called mirtrons, is carried out by the splicing machinery rather than Drosha (Okamura et al., 2007; Ruby et al., 2007). Therefore, expression of a mirtron is positively regulated by the splicing machinery, and, like the processing of canonical intronic miRNAs, the mature mRNA and mature miRNA can both be generated from the same transcript (Shomron and Levy, 2009). In contrast, the miRNAs that overlap splice sites of alternative exons can be produced only if the exon is not incorporated into the spliced mRNA molecule (Figure 7). In plants, primary miRNA transcripts undergo complex patterns of AS; and AS events may be involved in miRNA biogenesis (Hirsch et al., 2006; Mica et al., 2010), although this remains to be thoroughly tested. Our results show that splicing of primary miRNA transcripts affects the biogenesis of miRNAs in various animal species, and this type of regulation of miR-412 has a biological role in adult and embryonic murine brain tissues.

In the recently described family of mirtron-like miRNAs, only the 5′ hairpin terminus coincides with a splice junction; splicing defines the 5′ end of the pre-miRNA and the exosome is responsible for removal of the 3′ tail (Flynt et al., 2010; Ladewig et al., 2012). Biogenesis of miRNAs that overlap 5′ss, like hsa-miR-202, is not facilitated by exosome-mediated trimming, as splicing cleaves within the pre-miRNA structure (Figures S7E–S7G). It was previously shown that local RNA secondary structure can modulate splice-site selection and AS; this structure can interfere with or activate splicing, depending on the splicing regulatory elements affected (Graveley, 2005; Hiller et al., 2007; Shepard and Hertel, 2008). It remains unclear whether this is a stochastic or regulated mechanism for splice site recognition. Our data showed that, in addition to secondary structure formation that occurs when a pre-miRNA stem-loop conceals a splice site, splicing of the corresponding alternative exon is regulated by the levels of Drosha and DGCR8.

A key finding of this study is that AS negatively regulates miR-412 maturation but does not affect the biogenesis of miRNAs within the same transcript that are either intronic or exonic. The effect of AS on miR-412 biogenesis is specific and is dependent on the binding of U1 snRNA to the 5′ss (Figures 2A–2D). The same impact (exon inclusion) was observed following

overexpression of the TIA1, a protein known to facilitate binding of U1 snRNA (Wang et al., 2010). The balance between cellular levels of Microprocessor components and TIA1 appears to determine the expression of miR-412. Recent studies revealed that several splicing factors regulate processing of pre-miRNA at the posttranscriptional level (Guil and Cáceres, 2007; Trabucchi et al., 2009; Wu et al., 2010). In contrast to the impact of splicing on the miRNAs studied here, however, the role of splicing factors was suggested to be independent of splicing.

Finally, we provide evidence of the biological role of the mechanism described here. We demonstrate that miR-412 is active in neuronal cells and promotes efficient targeting of mRNAs into the RISC. We identified many mRNAs that are potential targets of the miRNA and validated several. We found that four putative miR-412 targets are integrated in a molecular network of proteins that are predominantly active in neuronal cell death processes. Notably, the splicing factor TIA1 promotes apoptosis (Förch et al., 2000), suggesting that regulation of miR-412 biogenesis by AS has a bona fide biological role. To conclude, our study found an intriguing competition between two nuclear RNA processing mechanisms, miRNA processing and RNA splicing, and demonstrated the implications of this interplay on miRNA and mRNA maturation in different tissues and developmental stages.

EXPERIMENTAL PROCEDURES

Detailed experimental procedures can be found in the Supplemental Experimental Procedures.

Plasmids

The mmu-miR-412, hsa-miR-202, and hsa-miR-365 minigenes were generated by amplifying genomic fragments using PCR (primers are listed in the Supplemental Experimental Procedures). Each primer contained an extension encoding a restriction enzyme sequence. PCR was performed using the Expand High Fidelity PCR System (Roche), and products were restriction digested and ligated into digested pEGFP-C3 vectors containing the CMV-IE promoter using T4 DNA Ligase (New England BioLabs) at 37°C for 2 hr. All clones were verified by sequencing. The pCK-Flag-Drosha plasmid and pCK-Flag-DGCR8 plasmid were kindly provided by V. Narry Kim (Seoul University). The AGO2 plasmid was kindly provided by Dr. Sven Diederichs (German Cancer Research Center [DKFZ]).

Cell Culture and Transfection Experiments

293T and N2A cells were cultured in Dulbecco's modified Eagle's medium supplemented with 4.5 g/ml glucose, 100 U/ml penicillin, 0.1 mg/ml streptomycin (Biological Industries), and 10% fetal bovine serum. Cells were cultured in six-well plates and grown to 60% confluence. Transfection was carried out using Mirus Bio's *Trans*IT-LT1 transfection reagent with 0.5 μg or 0.2 μg of plasmid DNA. RNA was harvested after 48 hr. Cells were transfected with siRNA against *drosha* mRNA (5′ GACCAGACUUUGUACCCUUTT 3′) or with a nonrelated scrambled siRNA (Ambion) to a final concentration of 60 nM in two rounds, 2 hr and 24 hr from initial cell split, using HiPerFect transfection reagent (QIAGEN).

SUPPLEMENTAL INFORMATION

Supplemental Information includes Supplemental Results and Discussion, Supplemental Experimental Procedures, seven figures, and three tables and can be found with this article online at http://dx.doi.org/10.1016/j.molcel.2013.05.007.

ACKNOWLEDGMENTS

The FLAG-Drosha plasmid and the FLAG-DGCR8 plasmid were kind gifts from Dr. V. Narry Kim (Seoul University). The AGO2 plasmid was kindly provided by Dr. Sven Diederichs (German Cancer Research Center [DKFZ]). We thank Dr. Noam Shomron and Dr. Schraga Schwartz and for comments and critical reading of the manuscript. We thank Mr. Dror Hollander for valuable input into this study. We thank Dr. Rani Elkon for statistical advice. G.A. and S.K. were supported by a grant from the Israel Science Foundation (ISF-BIkura 838/10). G.A. was funded by grants from the Israel Science Foundation (ISF) (ISF 61/09), ISF-Morasha 64/12, the Israel Cancer Association, and the Israel Cancer Research Foundation. S.K. was supported by ISF 1015/10 and a Marie Curie International Reintegration Grant. A.L. is grateful to the Azrieli Foundation for the award of an Azrieli Fellowship. N.A. was supported in part by a fellowship from the Edmond J. Safra Center for Bioinformatics at Tel Aviv University. R.S. was supported by a research grant from the ISF (Grant No. 241/11). The funders had no role in study design, data collection and analysis, decision to publish, or preparation of the manuscript.

Received: January 4, 2013
Revised: March 25, 2013
Accepted: April 30, 2013
Published: June 6, 2013

REFERENCES

Barash, Y., Calarco, J.A., Gao, W., Pan, Q., Wang, X., Shai, O., Blencowe, B.J., and Frey, B.J. (2010). Deciphering the splicing code. Nature *465*, 53–59.

Bartel, D.P. (2009). MicroRNAs: target recognition and regulatory functions. Cell *136*, 215–233.

Baskerville, S., and Bartel, D.P. (2005). Microarray profiling of microRNAs reveals frequent coexpression with neighboring miRNAs and host genes. RNA *11*, 241–247.

Braunschweig, U., Gueroussov, S., Plocik, A.M., Graveley, B.R., and Blencowe, B.J. (2013). Dynamic integration of splicing within gene regulatory pathways. Cell *152*, 1252–1269.

Buratti, E., and Baralle, D. (2010). Novel roles of U1 snRNP in alternative splicing regulation. RNA Biol. *7*, 412–419.

Cai, X., Hagedorn, C.H., and Cullen, B.R. (2004). Human microRNAs are processed from capped, polyadenylated transcripts that can also function as mRNAs. RNA *10*, 1957–1966.

Chiang, H.R., Schoenfeld, L.W., Ruby, J.G., Auyeung, V.C., Spies, N., Baek, D., Johnston, W.K., Russ, C., Luo, S., Babiarz, J.E., et al. (2010). Mammalian microRNAs: experimental evaluation of novel and previously annotated genes. Genes Dev. *24*, 992–1009.

Chong, M.M., Zhang, G., Cheloufi, S., Neubert, T.A., Hannon, G.J., and Littman, D.R. (2010). Canonical and alternate functions of the microRNA biogenesis machinery. Genes Dev. *24*, 1951–1960.

Curtin, J.F., and Cotter, T.G. (2004). JNK regulates HIPK3 expression and promotes resistance to Fas-mediated apoptosis in DU 145 prostate carcinoma cells. J. Biol. Chem. *279*, 17090–17100.

Del Gatto-Konczak, F., Bourgeois, C.F., Le Guiner, C., Kister, L., Gesnel, M.C., Stévenin, J., and Breathnach, R. (2000). The RNA-binding protein TIA-1 is a novel mammalian splicing regulator acting through intron sequences adjacent to a 5′ splice site. Mol. Cell. Biol. *20*, 6287–6299.

Denli, A.M., Tops, B.B., Plasterk, R.H., Ketting, R.F., and Hannon, G.J. (2004). Processing of primary microRNAs by the Microprocessor complex. Nature *432*, 231–235.

Filipowicz, W., Bhattacharyya, S.N., and Sonenberg, N. (2008). Mechanisms of post-transcriptional regulation by microRNAs: are the answers in sight? Nat. Rev. Genet. *9*, 102–114.

Flynt, A.S., Greimann, J.C., Chung, W.J., Lima, C.D., and Lai, E.C. (2010). MicroRNA biogenesis via splicing and exosome-mediated trimming in Drosophila. Mol. Cell *38*, 900–907.

Förch, P., Puig, O., Kedersha, N., Martínez, C., Granneman, S., Séraphin, B., Anderson, P., and Valcárcel, J. (2000). The apoptosis-promoting factor TIA-1 is a regulator of alternative pre-mRNA splicing. Mol. Cell *6*, 1089–1098.

Gal-Mark, N., Schwartz, S., Ram, O., Eyras, E., and Ast, G. (2009). The pivotal roles of TIA proteins in 5′ splice-site selection of alu exons and across evolution. PLoS Genet. *5*, e1000717.

Gdynia, G., Lehmann-Koch, J., Sieber, S., Tagscherer, K.E., Fassl, A., Zentgraf, H., Matsuzawa, S., Reed, J.C., and Roth, W. (2008). BLOC1S2 interacts with the HIPPI protein and sensitizes NCH89 glioblastoma cells to apoptosis. Apoptosis *13*, 437–447.

Golan, D., Levy, C., Friedman, B., and Shomron, N. (2010). Biased hosting of intronic microRNA genes. Bioinformatics *26*, 992–995.

Graveley, B.R. (2005). Mutually exclusive splicing of the insect Dscam pre-mRNA directed by competing intronic RNA secondary structures. Cell *123*, 65–73.

Griffiths-Jones, S., Saini, H.K., van Dongen, S., and Enright, A.J. (2008). miRBase: tools for microRNA genomics. Nucleic Acids Res. *36*(Database issue), D154–D158.

Guil, S., and Cáceres, J.F. (2007). The multifunctional RNA-binding protein hnRNP A1 is required for processing of miR-18a. Nat. Struct. Mol. Biol. *14*, 591–596.

Han, J., Lee, Y., Yeom, K.H., Kim, Y.K., Jin, H., and Kim, V.N. (2004). The Drosha-DGCR8 complex in primary microRNA processing. Genes Dev. *18*, 3016–3027.

Han, J., Lee, Y., Yeom, K.H., Nam, J.W., Heo, I., Rhee, J.K., Sohn, S.Y., Cho, Y., Zhang, B.T., and Kim, V.N. (2006). Molecular basis for the recognition of primary microRNAs by the Drosha-DGCR8 complex. Cell *125*, 887–901.

Han, J., Pedersen, J.S., Kwon, S.C., Belair, C.D., Kim, Y.K., Yeom, K.H., Yang, W.Y., Haussler, D., Blelloch, R., and Kim, V.N. (2009). Posttranscriptional crossregulation between Drosha and DGCR8. Cell *136*, 75–84.

Han, Z., He, H., Zhang, F., Huang, Z., Liu, Z., Jiang, H., and Wu, Q. (2012). Spatiotemporal expression pattern of Mirg, an imprinted non-coding gene, during mouse embryogenesis. J. Mol. Histol. *43*, 1–8.

Heo, I., Joo, C., Kim, Y.K., Ha, M., Yoon, M.J., Cho, J., Yeom, K.H., Han, J., and Kim, V.N. (2009). TUT4 in concert with Lin28 suppresses microRNA biogenesis through pre-microRNA uridylation. Cell *138*, 696–708.

Hiller, M., Zhang, Z., Backofen, R., and Stamm, S. (2007). Pre-mRNA secondary structures influence exon recognition. PLoS Genet. *3*, e204.

Hirsch, J., Lefort, V., Vankersschaver, M., Boualem, A., Lucas, A., Thermes, C., d'Aubenton-Carafa, Y., and Crespi, M. (2006). Characterization of 43 non-protein-coding mRNA genes in Arabidopsis, including the MIR162a-derived transcripts. Plant Physiol. *140*, 1192–1204.

Janas, M.M., Khaled, M., Schubert, S., Bernstein, J.G., Golan, D., Veguilla, R.A., Fisher, D.E., Shomron, N., Levy, C., and Novina, C.D. (2011). Feed-forward microprocessing and splicing activities at a microRNA-containing intron. PLoS Genet. *7*, e1002330.

Kadener, S., Rodriguez, J., Abruzzi, K.C., Khodor, Y.L., Sugino, K., Marr, M.T., 2nd, Nelson, S., and Rosbash, M. (2009). Genome-wide identification of targets of the drosha-pasha/DGCR8 complex. RNA *15*, 537–545.

Kanehisa, M., and Goto, S. (2000). KEGG: Kyoto encyclopedia of genes and genomes. Nucleic Acids Res. *28*, 27–30.

Karginov, F.V., Cheloufi, S., Chong, M.M., Stark, A., Smith, A.D., and Hannon, G.J. (2010). Diverse endonucleolytic cleavage sites in the mammalian transcriptome depend upon microRNAs, Drosha, and additional nucleases. Mol. Cell *38*, 781–788.

Kataoka, N., Fujita, M., and Ohno, M. (2009). Functional association of the Microprocessor complex with the spliceosome. Mol. Cell. Biol. *29*, 3243–3254.

Keren-Shaul, H., Lev-Maor, G., and Ast, G. (2013). Pre-mRNA splicing is a determinant of nucleosome organization. PLoS ONE *8*, e53506.

Kim, V.N. (2005). MicroRNA biogenesis: coordinated cropping and dicing. Nat. Rev. Mol. Cell Biol. *6*, 376–385.

Kim, Y.K., and Kim, V.N. (2007). Processing of intronic microRNAs. EMBO J. *26*, 775–783.

Kornblihtt, A.R. (2007). Coupling transcription and alternative splicing. Adv. Exp. Med. Biol. *623*, 175–189.

Krol, J., Loedige, I., and Filipowicz, W. (2010). The widespread regulation of microRNA biogenesis, function and decay. Nat. Rev. Genet. *11*, 597–610.

Ladewig, E., Okamura, K., Flynt, A.S., Westholm, J.O., and Lai, E.C. (2012). Discovery of hundreds of mirtrons in mouse and human small RNA data. Genome Res. *22*, 1634–1645.

Le Guiner, C., Lejeune, F., Galiana, D., Kister, L., Breathnach, R., Stévenin, J., and Del Gatto-Konczak, F. (2001). TIA-1 and TIAR activate splicing of alternative exons with weak 5′ splice sites followed by a U-rich stretch on their own pre-mRNAs. J. Biol. Chem. *276*, 40638–40646.

Lee, Y., Kim, M., Han, J., Yeom, K.H., Lee, S., Baek, S.H., and Kim, V.N. (2004). MicroRNA genes are transcribed by RNA polymerase II. EMBO J. *23*, 4051–4060.

Levy, C., Khaled, M., Robinson, K.C., Veguilla, R.A., Chen, P.H., Yokoyama, S., Makino, E., Lu, J., Larue, L., Beermann, F., et al. (2010). Lineage-specific transcriptional regulation of DICER by MITF in melanocytes. Cell *141*, 994–1005.

Liang, H., and Li, W.H. (2007). MicroRNA regulation of human protein protein interaction network. RNA *13*, 1402–1408.

Long, J.C., and Caceres, J.F. (2009). The SR protein family of splicing factors: master regulators of gene expression. Biochem. J. *417*, 15–27.

Luco, R.F., Allo, M., Schor, I.E., Kornblihtt, A.R., and Misteli, T. (2011). Epigenetics in alternative pre-mRNA splicing. Cell *144*, 16–26.

Lund, E., Güttinger, S., Calado, A., Dahlberg, J.E., and Kutay, U. (2004). Nuclear export of microRNA precursors. Science *303*, 95–98.

Macias, S., Plass, M., Stajuda, A., Michlewski, G., Eyras, E., and Cáceres, J.F. (2012). DGCR8 HITS-CLIP reveals novel functions for the Microprocessor. Nat. Struct. Mol. Biol. *19*, 760–766.

Mercer, T.R., Dinger, M.E., Sunkin, S.M., Mehler, M.F., and Mattick, J.S. (2008). Specific expression of long noncoding RNAs in the mouse brain. Proc. Natl. Acad. Sci. USA *105*, 716–721.

Mica, E., Piccolo, V., Delledonne, M., Ferrarini, A., Pezzotti, M., Casati, C., Del Fabbro, C., Valle, G., Policriti, A., Morgante, M., et al. (2010). Correction: High throughput approaches reveal splicing of primary microRNA transcripts and tissue specific expression of mature microRNAs in Vitis vinifera. BMC Genomics *11*, 109.

Morlando, M., Ballarino, M., Gromak, N., Pagano, F., Bozzoni, I., and Proudfoot, N.J. (2008). Primary microRNA transcripts are processed co-transcriptionally. Nat. Struct. Mol. Biol. *15*, 902–909.

Okamura, K., Hagen, J.W., Duan, H., Tyler, D.M., and Lai, E.C. (2007). The mirtron pathway generates microRNA-class regulatory RNAs in Drosophila. Cell *130*, 89–100.

Pawlicki, J.M., and Steitz, J.A. (2008). Primary microRNA transcript retention at sites of transcription leads to enhanced microRNA production. J. Cell Biol. *182*, 61–76.

Peritz, T., Zeng, F., Kannanayakal, T.J., Kilk, K., Eiríksdóttir, E., Langel, U., and Eberwine, J. (2006). Immunoprecipitation of mRNA-protein complexes. Nat. Protoc. *1*, 577–580.

Ries, V., Silva, R.M., Oo, T.F., Cheng, H.C., Rzhetskaya, M., Kholodilov, N., Flavell, R.A., Kuan, C.Y., Rakic, P., and Burke, R.E. (2008). JNK2 and JNK3 combined are essential for apoptosis in dopamine neurons of the substantia nigra, but are not required for axon degeneration. J. Neurochem. *107*, 1578–1588.

Roca, X., Krainer, A.R., and Eperon, I.C. (2013). Pick one, but be quick: 5′ splice sites and the problems of too many choices. Genes Dev. *27*, 129–144.

Rodriguez, A., Griffiths-Jones, S., Ashurst, J.L., and Bradley, A. (2004). Identification of mammalian microRNA host genes and transcription units. Genome Res. *14*(10A), 1902–1910.

Ruby, J.G., Jan, C.H., and Bartel, D.P. (2007). Intronic microRNA precursors that bypass Drosha processing. Nature *448*, 83–86.

Saini, H.K., Griffiths-Jones, S., and Enright, A.J. (2007). Genomic analysis of human microRNA transcripts. Proc. Natl. Acad. Sci. USA *104*, 17719–17724.

Satoh, J. (2012). Molecular network of microRNA targets in Alzheimer's disease brains. Exp. Neurol. *235*, 436–446.

Shepard, P.J., and Hertel, K.J. (2008). Conserved RNA secondary structures promote alternative splicing. RNA *14*, 1463–1469.

Shomron, N., and Levy, C. (2009). MicroRNA-biogenesis and Pre-mRNA splicing crosstalk. J. Biomed. Biotechnol. *2009*, 594678.

Siomi, H., and Siomi, M.C. (2010). Posttranscriptional regulation of microRNA biogenesis in animals. Mol. Cell *38*, 323–332.

Tardy, C., Sabourdy, F., Garcia, V., Jalanko, A., Therville, N., Levade, T., and Andrieu-Abadie, N. (2009). Palmitoyl protein thioesterase 1 modulates tumor necrosis factor alpha-induced apoptosis. Biochim. Biophys. Acta *1793*, 1250–1258.

Trabucchi, M., Briata, P., Garcia-Mayoral, M., Haase, A.D., Filipowicz, W., Ramos, A., Gherzi, R., and Rosenfeld, M.G. (2009). The RNA-binding protein KSRP promotes the biogenesis of a subset of microRNAs. Nature *459*, 1010–1014.

Wang, D., Lu, M., Miao, J., Li, T., Wang, E., and Cui, Q. (2009). Cepred: predicting the co-expression patterns of the human intronic microRNAs with their host genes. PLoS ONE *4*, e4421.

Wang, Z., Kayikci, M., Briese, M., Zarnack, K., Luscombe, N.M., Rot, G., Zupan, B., Curk, T., and Ule, J. (2010). iCLIP predicts the dual splicing effects of TIA-RNA interactions. PLoS Biol. *8*, e1000530.

Winter, J., Jung, S., Keller, S., Gregory, R.I., and Diederichs, S. (2009). Many roads to maturity: microRNA biogenesis pathways and their regulation. Nat. Cell Biol. *11*, 228–234.

Wu, H., Sun, S., Tu, K., Gao, Y., Xie, B., Krainer, A.R., and Zhu, J. (2010). A splicing-independent function of SF2/ASF in microRNA processing. Mol. Cell *38*, 67–77.

Yan, K., Liu, P., Wu, C.A., Yang, G.D., Xu, R., Guo, Q.H., Huang, J.G., and Zheng, C.C. (2012). Stress-induced alternative splicing provides a mechanism for the regulation of microRNA processing in Arabidopsis thaliana. Mol. Cell *48*, 521–531.

Yi, R., Qin, Y., Macara, I.G., and Cullen, B.R. (2003). Exportin-5 mediates the nuclear export of pre-microRNAs and short hairpin RNAs. Genes Dev. *17*, 3011–3016.

Yosef, N., Zalckvar, E., Rubinstein, A.D., Homilius, M., Atias, N., Vardi, L., Berman, I., Zur, H., Kimchi, A., Ruppin, E., and Sharan, R. (2011). ANAT: a tool for constructing and analyzing functional protein networks. Sci. Signal. *4*, pl1.